Ore and Energy Resource Geology 8 (2021) 100014

Contents lists available at ScienceDirect

Ore and Energy Resource Geology

journal homepage: www.sciencedirect.com/journal/ore-and-energy-resource-geology

Gold occurrences in copper-magnetite-apatite deposit at Seruwila, Sri Lanka

Nishika Samarakoon [a,b], Sanjeewa P.K. Malaviarachchi [a,b,*], Atula Senaratne [a], Athula Wijayasinghe [b]

[a] Department of Geology, Faculty of Science, University of Peradeniya, Sri Lanka
[b] National Institute of Fundamental Studies, Hantna Road, Kandy, Sri Lanka

ARTICLE INFO

Keywords:
Gold
Kiruna-type deposits
Copper–iron oxide–apatite
Gondwana
Sri Lanka

ABSTRACT

This study presents petrology and evidence for possible gold occurrences in Seruwila copper–iron oxide–apatite (IOA) deposit, hosted in an ultramafic intrusion which is located at the boundary between the Highland and Vijayan complexes, within the intermediate-granitic basement in north-eastern Sri Lanka. The study is complemented with petrological observations and XRD and SEM analysis, respectively, to investigate the petrology/subsurface geology of the deposit and identify possible gold occurrences in the deposit. The ore-bearing rocks are mainly composed of magnetite and apatite in various proportions, hosted in an ultramafic intrusion with cumulate features within the granitic-intermediate basement. The secondary veins contain magnetite, chalcopyrite, pyrrhotite, and pyrite together with apatite and scapolite, tremolite, diopside, and minor actinolite and calcite, serpentinite, anhydrite, or gypsum. The clinopyroxene euhedral crystals show cumulus textures including grain triple junctions and large dihedral angles (~120°), showing magmatic origin. Texturally two types of amphiboles are identified as coarse-grained (0.5–1 mm), pale green euhedral amphibole that is free of inclusions, and fine-grained (<0.1 mm) and brownish, occurring as anhedral inclusions in clinopyroxene. The deposit contains varying amounts of sulfides in which pyrite is the potential gold carrier in magmatic–hydrothermal processes. By the results of XRD analysis, it is evident that the presence of Au (111), Au (200), Au (220) and Au (311), although with low count values (50–500), probably due to the low concentration of gold. Therefore, particularly in the samples with veins or veinlets, gold was inferred to be present in pyrite/chalcopyrite as invisible structurally-bonded gold and/or gold nanoparticles. Hence, the results of this study, although at non-ore grade, veinlets of gold-bearing pyrite/chalcopyrite may serve as a promising target for gold occurrence, being a potential site of gold-mineralization in the context of the East-Gondwana.

1. Introduction

The economic interest of iron oxide-apatite (IOA) deposits is due to their mineable quantities of magnetite, hematite and variable amounts of P, Cu, Au, Ag, REE, U, and Co ([6,42,102]). After the classification by [34], iron oxide–apatite deposits have gained exploration and research interest worldwide. These deposits show a wide variety of hydrothermal features, mineralization, time-space patterns, and their geophysical characteristics, suggesting that they are significant sources for Cu and Au. The origin of IOA deposits has remained controversial, although recent studies have suggested an integrated magmatic–hydrothermal model (e.g., [49,89,93,8],57]). This model confirms the genetic connection between Kiruna-type IOA and iron oxide–copper–gold (IOCG) deposits, in which IOA deposits represent the deeper roots of the IOCG systems (e.g., [87,23]).

Kiruna-type IOA deposits occur in various tectonic settings such as Sweden, Iran, American Cordillera, and China [31,38,41,77,32]. The presence of these deposits in ultramafic rocks are rare, and most of them are small-scale deposits. Few deposits have been reported comprising fluoro-hydroxyl-apatite associated with chlorite-talc schists located in the margin of small ultramafic bodies in Georgia and Maryland, U.S.A. [31], and low concentrations of magnetite–apatite rocks in ophiolite complexes (e.g. Orthys Complex, Greece and Lizard Complex, U.K., [66, 37,39]).

Gold may have occurred in three ways in these deposits. The first one is elemental gold crystallized in micro veins and cavities (as inclusions) inside the pyrite and chalcopyrite grains, characterizing its hydrothermal alteration. The second one is a small amount of gold occur by

* Corresponding author.

https://doi.org/10.1016/j.oreoa.2021.100014
Received 18 June 2021; Accepted 17 August 2021
Available online 18 August 2021

coupled substitutions within pyrite. The third way is the presence of Au precipitates on the Fe_3O_4 surface. According to Richard Diaz et al.,2010, The SEM-EDX and BSE analyses of the magnetite particles after treatment reported the presence of Au cements or Au precipitates on magnetite surface and it was influenced by pH, contact time, chloride concentration, and initial Au concentration. The detected gold appeared as a cluster of Au cement or precipitates.

Pyrite is the most important sulfide mineral and occurs in various tectonic settings, including sedimentary and metamorphic rocks [26]. Pyrites usually distributing in veins and fractures in the rock. Pyrite develops in a later phase of mineralization with the introduction of hydrothermal fluids. Generally, the concentration of trace elements distributed in pyrite depends on the content in parent fluids ([98]), refractory nature in pyrite [26] and environmental conditions during the recrystallization of pyrite. Pyrite is a dominant gold carrier in many types of ore deposits, according to previous works [2,3,10,88,101]. In pyrite, gold can be present either as visible grains [1,4,5] or as invisible grains recognized by micro-beam analytical tools [69,70,88,94]. The invisible gold can be structurally bound gold and/or gold nanoparticles [26,30,88,92]. Sometimes, the presence of invisible gold in pyrite is considered to be a result of the substitution of Au(I) for Fe and/or S in the structure of As-poor pyrite. Generally, there are three opinions about the valence state of structurally bound gold in pyrite: Au^{1-} substituting for S^{1-}, Au^{3+} substituting for Fe^{2+} [2,3] and Au^{1+} substituting for Fe^{2+} [69]. However, other studies have shown that arsenic may not be essential to enrich gold in pyrite, but other elements such as Te or Bi may be a significant gold scavenger in As-deficient hydrothermal systems (e.g. [10]).

Gold-bearing mineral deposits contain varying amounts of sulfides in which pyrite is the dominant gold carrier in magmatic–hydrothermal processes. Recent petrological and geochemical studies have suggested, this deposit is a Kiruna-type IOA deposit and it was originated by

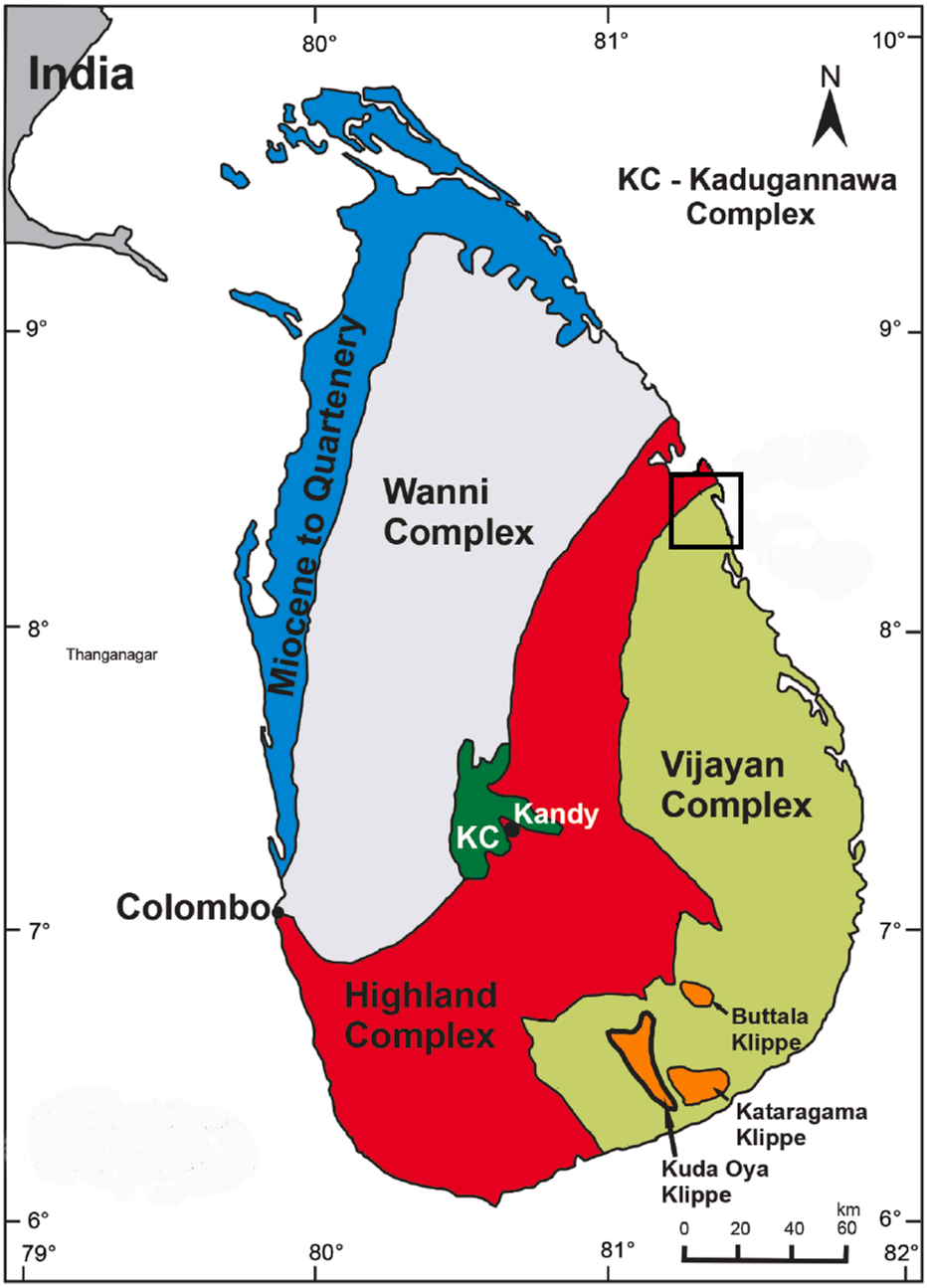

Fig. 1. Geological and tectonic framework of Sri Lanka showing the major crustal blocks, their boundaries. (Modified after [16], and [27].).

magmatic–hydrothermal processes [28]. In this study, we present the petrology, textual and compositional data of hydrothermal pyrite in ultramafic rock, occurrence, and distribution of gold. The main goal of this paper is to introduce possible gold occurrences in this deposit based on analytical results of petrography, XRD, and SEM data. In these systems, gold may be transported primarily as sulfide complexes, with gold being deposited in response to mixing of the deep hydrothermal fluids. Abundant gold bearing pyrite may be precipitated in the ultramafic rocks and primarily occurring as veinlets, disseminations and fine-grained aggregates.

2. General geology of Sri Lanka

Sri Lanka is a small crustal fragment of eastern Gondwana. Majority of rocks in the Sri Lankan basement (more than 90%) comprises of highly crystalline, non fossilfereous high grade metamorphic rocks of more than 570 Ma from the Precambrian era. The rest comprises sedimentary formations such as limestone, sand and clay of the Jurassic period (Thabbowa, Andigama, Pallama), tertiary, and quaternary periods. In the northern zone, a layer of limestone formed during the Miocene epoch [16,53]. Except these, there are several rocks have igneous origin such as carbonatites, dolerite, granites, and pegmatites. The metamorphic basement of Sri Lanka is subdivided into four tectonic units (Fig. 1) based on crustal formation by Nd model age determinations ([62]), metamorphic grade, lithology and structures [169]. These are Highland Complex (HC), Wanni Complex (WC), Vijayan Complex (VC), and Kadugannawa Complex(KC).

2.1. The Highland Complex

The HC represent the central belt of Sri Lanka which extended from northeast towards southwest direction belonging to the central highlands of the island. The HC contains metasedimentary and metaigneous rocks such as pelitic gneisses, quartzites, marbles, calc silicate rocks, metagranitoid, granitic gneisses, and charnockites ([104,16,60,72,81,85,86]). Additionally, in the central part and northern part of the HC, thick bands of marble and quartzites are observed about 40 km in length while in southwestern part of the HC, thick bands of marble and quartzites are rare and mappable thin bands of wollostonite, scapolite, diopside bearing calcsilicates, cordiorite bearing metapelitic gneisses and othogneisses are dominant rock types [72,74,78].

Rocks of Highland Complex were metamorphosed to regional granulite facies conditions [24,33,72,75,85]. The whole HC represent as a tilted metamorphic terrane, P-T gradient increases from about 4.5–6 kbar and 700–750 °C in southwestern part to 8–9 kbar and 800–900 °C in east and southeast ([24,75,85,51,11,50,61]). The extreme crustal metamorphism of HC occurred at 925–1150 °C and 9–12.5 kbar have been reported in several localities in the central part and rarely in the southwestern part of the HC ([50,67,68,20,59,80]).

The Highland Complex is the oldest lithotectonic unit, Nd model ages of 2.0 to 3.4 Ga obtained from the Highland Complex rocks with depleted mantle model and it was derived from late Archean sources [62]. This complex comprises a wide range of detrital zircon which are separated from metasediments and U-Pb ages of these zircons ranging from 3.2 to 2.0 Ga [35,36,56]. The peak metamorphism of HC rocks around 0.61–0.55 Ga [7,20,35,36,52,58,82,90,91] and othogneisses of HC yield a magmatic age of 2.0–1.8 Ga and 0.67 Ga ([36,52,56,82]).

2.2. The Vijayan Complex

The Vijayan Complex is dominantly composed of upper amphibolite to granulite facies rocks [16,27,29,43,55,61]. This unit consists mainly granitoid gneisses, augen-gneisses, migmatites, hornblende-biotite gneisses possibly derived from mafic dykes [15,43,55,61] and minor metasedimentary enclaves of quartzite, calc-silicate rocks and marble are also found [17,18,43,53,56].

Most of the hornblende-biotite granitoids range between diorite and granite with the dominant compositions being granodiorite and granite [47,53,63,64] and VC rocks originated at a subduction related tectonic environment by regional metamorphism and crustal anatexis [27,64,73,82]. The VC was metamorphosed at 580–550 Ma by crustal anatexis magmatism event that occurred during the early Neoproterozoic time [45,54,55]. In addition to few inliers which consisting of typical HC rocks occur at Katharagama, Kudaoya and buttala within VC and a mixed zone of rocks from both terranes in which garnet-bearing granulites are apparently restricted, where around the villages of Mahawalatenna, Wellawaya, Embilipitiya and Kirinda in southern Sri Lanka [27,55].

In the east around Mahiyangana and Pottuvil area, minor granulite-facies mineral assemblages (late-stage patchy charnockitization) are found in metadioritic to metagabbroic rocks [40,103]. Mafic dykes and minor gabbroic gneisses grow interlayered and infolded with granitoid gneisses. Additionally, pegmatites and pink granites also can be observed locally as the youngest intrusions. Vijayan rocks exhibit evidence of migmatization ([55]). The Vijayan Complex have Nd-ages of 1.1–3.3 Ga [62,63,103] with the depleted mantle model and the emplacement age of the protolith of the Vijayan gneisses were at 1000–1100 Ma [54,55]. The age of metamorphism of the VC has been interpreted as Zircon U-Pb ages of about 590–456 Ma [27,35,36,56].

2.3. The Wanni Complex

The Wanni Complex composed of an upper amphibolite to granulite facies metaigneous rocks and a minor amount of metasedimentary rocks ([75,84,7,14]). The metaigneous rocks are varying granitic, granodioritic, monzonitic, tonalitic, charnockitic and enderbitic in composition. The metasedimentary rocks comprise garnet-sillimanite gneisses, cordierite gneisses, quartzites and calcsilicates which are located as minor bands close to the western margin of the Highland Complex [43,73].

Migmatization is also distributed over a large area through the WC ([51]). Migmatites and cordierite bearing gneisses are dominant in Colombo and Gampaha areas and Charnockitic gneisses are rich in the northern lowlands where around Vavuniya [52], while arrested charnockites are common in few areas (e.g.: Anamaduwa and Kurunegala). The WC comprises apatite bearing unmetamorphosed carbonatite deposits in the northern WC where at Eppawala and Kawisigamuwa, and unmetamorphosed post-tectonic K-feldspar rich granite at Tonigala [16,35]. The WC has yielded Nd model age 2000–1000 Ma [62,63] and show a wide range of magmatic events reported by detrital zircon ages, four episodes of magmatism have been identified which are 1100–1000 Ma, 980–894 Ma, 790–750 Ma and 550 Ma [35,36,52,52,62,63,82].

2.4. The Kadugannawa Complex

The KC is formerly known as “Arenas” which was first identified and named by Coates in 1935 and it forms in large, doubly plunging synforms in the central part of the country [96]. This unit is dominated by hornblende and biotite bearing orthogneisses, gabbros, diorites, granodioritic to granitic gneisses, charnockites, enderbites and minor metasediments [46,54,100], and based on similarities in geochemical, structural and geochronological evidence suggested that the KC is a part of the WC [43,54].

The complex includes rocks were metamorphosed under upper amphibolite to granulite facies conditions ([16,53,58]) and estimated metamorphic conditions are 3.5–7.5kbar and 600– 900 °C ([24,84]. The KC has yielded Nd model ages ranging between 1600 and 1000 Ma [62,63]] and several thermal events have been recorded in the rocks of KC at 832, 780, 721, 661–605 Ma [29]. All KC rocks were metamorphosed during 610–500 Ma and charnockitisation was occurred at 590–535 Ma ([7,35,52,29,82]).

2.5. The Highland Vijayan tectonic boundary

The suture between the HC and VC was developed under subduction related tectonic settings.The HC is younger than other two complexes, which was suggested by few workers based on the field relations [21,65,71]. While the boundary between the VC and the HC is an important geological contact zone and it is suggested as a sub-horizontal ductile shear zone by many researchers [13,25,47,48,51,56,62,95,97]. This HC-VC shear zone was created by the already attached HC-WC block collided with the VC block (during late Neoproterozoic time), generated late upright folds and then ductile deformation and finally, resulted in thrust contact between VC and HC [43–45]. The amalgamation of Highland Complex and Vijayan Complex in a nearly E–W direction (present coordinates) was occurred during Pan-African plate convergence [44,45], and the final phase of suturing presumably produced thrust zone between VC and HC. The suturing is considered to slightly postdate the peak granulite-facies metamorphism in the HC [44,79].

The Highland Complex close to the boundary is dominated by charnockitic gneiss with the minor occurrences of garnet-biotite gneiss while the Vijayan Complex is dominated by hornblende biotite gneiss with minor occurrence of granitic gneiss. Iron and polymetallic mineral deposits form where the iron ores form as massive and well crystallized magnetite aggregates, and sometimes cover the whole hillock along the HC-VC boundary close to Buttala. Pyrite, chalcopyrite and bornite are also associated with iron ores. The HC-VC contact preserves evidence for specific rock associations and which was developed under subduction related tectonic settings comprising metachert, serpentinised ultramafic units, anorthosites and metabasalts [21,27]. Along the HC-VC boundary contains serpentinite bodies near Ussangoda [27,76], Cu-sulfide deposits [22], massive magnetite-hematite deposit at Wellawaya and IOA-type deposit at Seruwila [40]. HC-VC Observations can prove boundary rocks are deformed because intense deformation and migmatization are the predominant evidence for deformation of the boundary. Mylonites and migmatites are seen at many localities along the boundary shear zone, and it was formed due to the influx of aqueous fluids along the shear zones, and continuous suturing may have been responsible for mylonitization and migmatization. The boundary shear zone generated under granulite facies conditions and continued during retrogression to upper amphibolite facies conditions [47,48].

3. Study area, samples and methods

3.1. Iron oxide–apatite (IOA) deposit in Seruwila, Sri lanka

The study area is located along the tectonic contact between the Vijayan and Highland Complexes (Fig. 1). The first discovery of the IOA deposit at Seruwila by the Sri Lankan Geological Survey in 1971, during the systematic mapping program of the island. It has been revisited in several aspects such as geology and tectonic settings, mineral deposit model, classification as well as origin of the mineralization. The mineralization is hosted in an ultramafic intrusion. The IOA deposit at Seruwila has no world-class economic value because of its relatively small size compared to other copper-gold-iron deposits in the world. This deposit is a Kiruna-type IOA deposit and is regarded to be originated by magmatic–hydrothermal processes [28].

The Seruwila iron oxide apatite deposit comprises massive and scattered mineralization and it formed as well defined lenticular pods in host rock during the late Neoproterozoic time. The mineralization is cut across by a set of normal faults (Fig 2). The mineralization is hosted in ultrabasic rocks varying from 1 to 5 m in length and it originates as discontinuous and disrupted layers. The highly weathered surfaces of magnetite bearing ultramafic rocks comprise with secondary copper minerals such as malachite and azurite. The basement rock in Seruwila area is mainly clinopyroxene bearing meta-igneous rocks (enderbite) which produce a sharp contact with the magnetite bearing ultrabasic rocks [40].

At the margin of the mineralization, a layer of calc silicate rock and anorthosite occur in which coarse grained minerals are found [40]. Calcite, apatite, and olivine (fayalite) are the dominant minerals in the calc-silicate rock, while plagioclase with labradorite (Fig. 3) composition is dominant mineral in anorthosite [71]. Coarse scapolite grains occur in the ultrabasic rocks with up to 2 cm in length at transition zone. Sulfide minerals were occurred in secondary calc-silicate veins which can observed along fractures, while valleriite {(Cu FeS_2) (Mg Al Fe $(OH)_2$}, Smythite (51.1%Fe 45.2%S), serpentinite, anhydrite, or gypsum are also present in secondary veins [40].

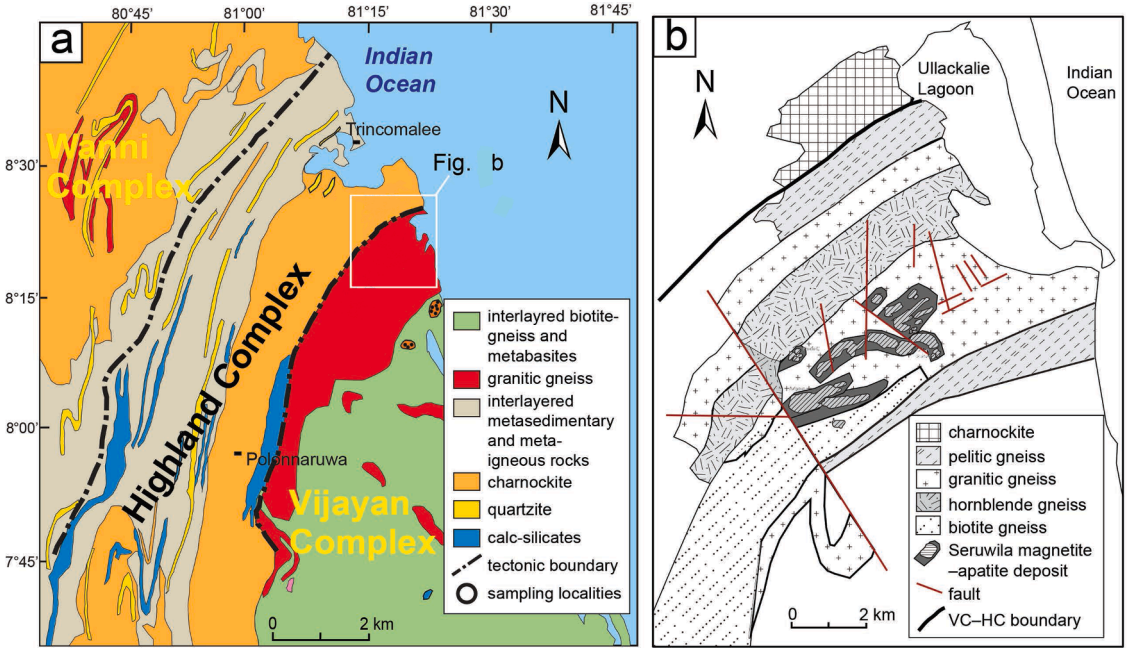

Fig. 2. (a) Detailed geological map of the study area showing the northern part of the boundary between Highland and Vijayan Complexes, together with sample localities. (Modified after [16]). (b) Geological map of Seruwila copper-magnetite deposit. (Modified after [83] and [12].).

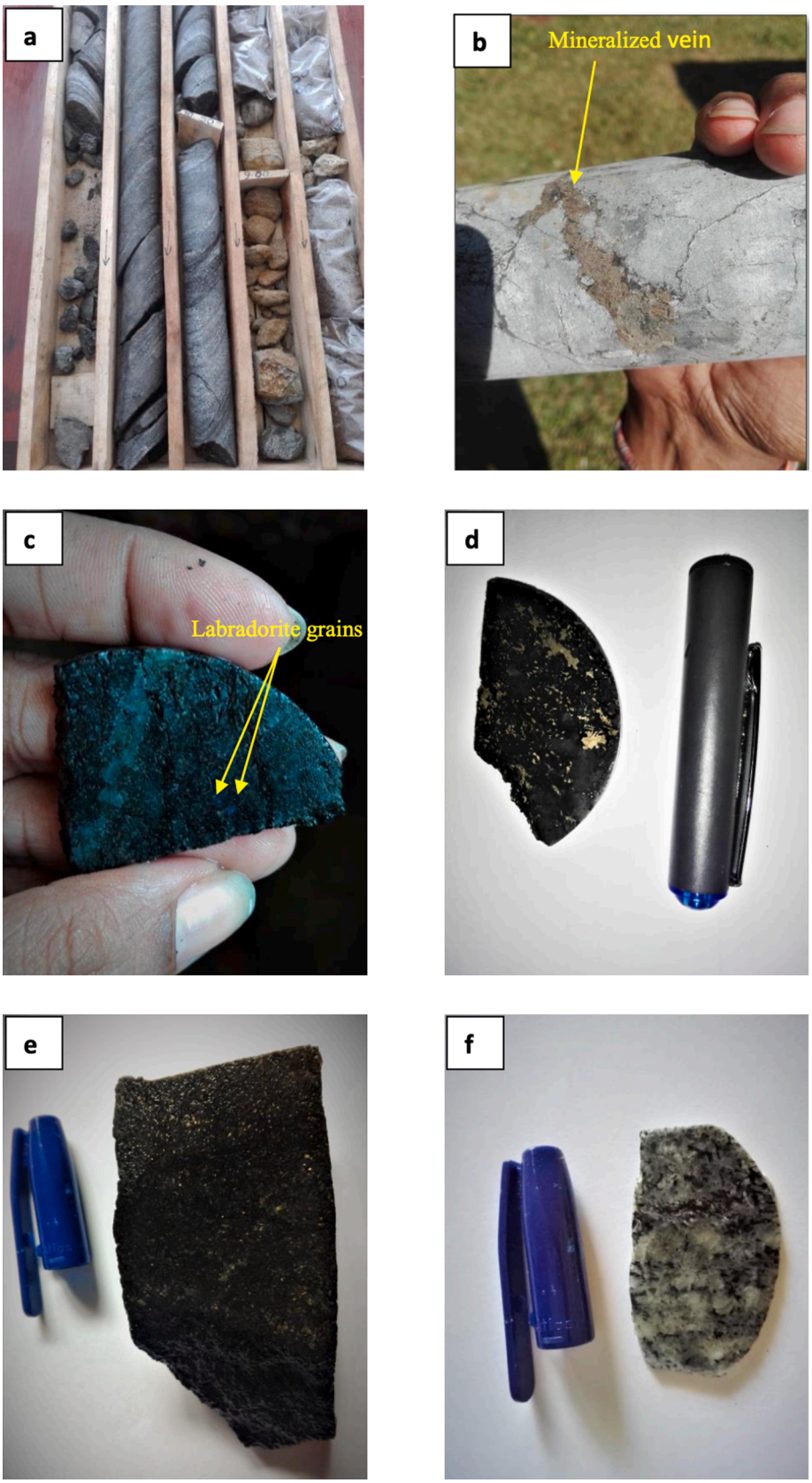

Fig. 3. (a)The oriented core samples in a wooden core tray. (b) Sulfide minerals rich veins in ultramafic rock. (c) Labradorite grains in ultramafic rock. (d) Mineralized host rock. (e) A sample of ultramafic rock. (f) A sample of intermediate. rock.

The ore mineralization at Seruwila can be subdivided into: (1) ultramafic host rock; (2) massive magnetite–apatite ore rock; (3) disseminated magnetite-apatite ore; (4) transitional zone ore-bearing ultramafic rock; and (5) clinopyroxene-bearing enderbitic basement rock [27]. Ultramafic host rock dominantly consists of medium to coarse-grained clinopyroxene, amphibole while fine-grained magnetite and apatite as the minor minerals. Massive magnetite–apatite ore rock is mainly composed of highly coarse grained magnetite (contains diopside inclusions) and apatite, and it vary from 1 to 10 m in length. The disseminated magnetite ores occurred the calc-silicate veins together with minor sulfides, and consist magnetite, chalcopyrite, pyrrhotite, and pyrite together with apatite and scapolite, tremolite, diopside as the major minerals with actinolite and calcite as minor minerals. The transitional zone ore-bearing ultramafic rocks comprise with generally medium to coarse-grained clinopyroxene, magnetite, amphibole, scapolite, and apatite with accessory hematite with equigranular massive texture.

3.2. Samples

The sampling location is at 80 23′ 22.6′′ N and 810 19′ 25.3′′ E (Coordinates of the drill hole). In this study, drill core samples were used for all laboratory analysis (Table 1). The host rock for mineralization is an ultramafic rock and a mineralized zone was observed from the depth of 28.00 m to 60.30 m. Drill core samples were collected and initially, these were studied by naked eye to identify visible petrological characteristics (Fig. 3). After careful studies in hand specimens, suitable samples were selected for thin section preparation based on the general geology, the changes in mineralization, textural variations, mineralogical variations and as best representation of mineralization zone of drill core etc. Core samples were selected for thin section preparation from the depth of 26.30 m to 61.10 m. Thin sections were prepared in the Petrology Laboratory, Department of Geology, University of Peradeniya (Sri Lanka) and, in the Petrology Laboratory, National Institute of Fundamental Studies, Kandy (Sri Lanka). Thirty thin sections were produced and they were used to study in detail mineral textures, reactions, alteration textures and other petrographic characteristics at the petrology laboratory using a standard petrographic microscope (Carl Zeiss).

Table 2

3.3. Methods

About a 25.0 cm long core to represent each meter of the mineralization was selected and sawed to split in half (Figs. 3 and 4). Selected samples were cleaned to prepare sample powders without contaminations. A half core with approximately 25 cm in length was crushed in a laboratory crusher and then the crushed rock was split using a splitter several times to get a reasonably sized sample for further grinding. Samples were selected for XRD analysis where it contains pyrite rich veins. A twelve representative samples were analyzed by XRD instruments at the National Institute of Fundamental Studies, Kandy (Sri Lanka) and Post Graduate Institute of Science, University of Peradeniya (Sri Lanka). The following operating conditions were maintained: radiation Co Kα (35 kV/40 mA); the speed of goniometer of 0.02° 2θ per step with a counting time of 1.0 s per step and collected 20–80° 2θ. For the XRD analysis at the NIFS, the conditions used were: Cu Kα (30 kV/49 mA); the speed of goniometer of 0.020 2θ per step with a counting time of 1.0 s per step and collected 10–80° 2θ.

The Scanning Electron Microscope (SEM) analyses were mainly performed to identify possible gold occurrences in the studied samples. Five suitable thin sections were selected which consisted of pyrite rich veins. That selected five thin sections were polished with the diamond paste using the diamond polisher (Model no STG/R-054/01) at the petrology lab of NIFS, Kandy (Sri Lanka). Then, thin sections were cut to remove any extra portions to get the standard size for SEM analysis. Initially, selected thin sections with standard size were coated with carbon coating. Subsequently, carbon coated thin sections were placed in (SEM) instrument and analysis were carried out. Analyses were carried out on Hitachi SU6600 Analytical Variable Pressure FE-SEM (Field Emission Scanning Electron Microscope) at SLINTEC academy, Homagama, Sri Lanka. Samples were mounted onto the sample stub using carbon tapes and the images were taken at 15 kV both in secondary and backscattered modes. EDS: Spectra were recorded at 15 kV. WDS: Spectra were recorded at 20 kV.

Inductively Coupled Plasma Mass Spectrometer (ICP-MS) by ICAPQ (Thermo Fisher) was used to determine the trace elements and Rare Earth Element (REE) concentrations in the Geochemistry Laboratory of Department of Geology, University of Peradeniya, Peradeniya, Sri

Table 1
List of samples referred with the depth of the drill-core.

Sample No.	with Drill Core depth (m)	Rock type
SW-1	26.30	Metamorphosed granitic rock
SW-2	27.00	Metamorphosed granitic rock
SW-3	29.50	Metamorphosed granitic rock
SW-4	30.65	Metamorphosed Intermediate basement rock (enderbitic)
SW-5	31.70	Metamorphosed Intermediate basement rock (enderbitic)
SW-6	33.20	Metamorphosed Intermediate basement rock (enderbitic)
SW-7	34.30	Metamorphosed Intermediate basement rock (enderbitic)
SW-8	35.10	Ore bearing Ultramafic rock
SW-9	36.00	Metamorphosed Ultramafic host rock
SW-10	37.30	Ore bearing Ultramafic rock
SW-11	38.30	Ore bearing Ultramafic rock
SW-12	39.60	Ore bearing Ultramafic rock
SW-13	40.84	Metamorphosed Intermediate basement rock (enderbitic)
SW-14	41.15	Metamorphosed Intermediate basement rock (enderbitic)
SW-15	42.85	Metamorphosed Intermediate basement rock (enderbitic)
SW-16	43.80	Metamorphosed Intermediate basement rock (enderbitic)
SW-17	44.60	Metamorphosed Intermediate basement rock (enderbitic)
SW-18	45.30	Metamorphosed Intermediate basement rock (enderbitic)
SW-19	46.70	Metamorphosed Intermediate basement rock (enderbitic)
SW-20	47.50	Metamorphosed Intermediate basement rock (enderbitic)
SW-21	48.10	Metamorphosed Intermediate basement rock (enderbitic)
SW-22	50.00	Metamorphosed Intermediate basement rock (enderbitic)
SW-23	50.80	Metamorphosed Intermediate basement rock (enderbitic)
SW-24	51.80	Metamorphosed Intermediate basement rock (enderbitic)
SW-25	53.61	Metamorphosed Intermediate basement rock (enderbitic)
SW-26	54.50	Metamorphosed Intermediate basement rock (enderbitic)
SW-27	55.60	Metamorphosed Intermediate basement rock (enderbitic)
SW-28	56.90	Metamorphosed Intermediate basement rock (enderbitic)
SW-29	57.50	Metamorphosed Intermediate basement rock (enderbitic)
SW-30	58.40	Metamorphosed Intermediate basement rock (enderbitic)
SW-31	59.00	Metamorphosed Intermediate basement rock (enderbitic)
SW-32	60.00	Metamorphosed Intermediate basement rock (enderbitic)
SW-33	61.10	Metamorphosed Intermediate basement rock (enderbitic)

Table 2
Important ore-trace elements observed in the studied samples.

Depth	Co (ppm)	Ni (ppm)	Cu (ppm)	Zn (ppm)	Cr (ppm)	Mn (ppm)	Fe%
27.00 m	51.77	169.56	266.77	89.88	107.33	591.62	10.74
28.30 m	17.61	29.48	60.04	64.13	82.82	494.25	6.92
29.50 m	42.53	111.81	127.72	66.04	414.98	682.78	7.44
30.65 m	46.32	86.93	154.53	69.14	154.22	659.54	9.56
31.70 m	42.38	136.54	277.26	93.54	131.56	414.65	11.55
35.20 m	47.04	67.00	159.28	76.21	67.25	406.62	7.43
34.30 m	47.63	77.04	132.25	75.88	119.10	700.32	9.23
35.10 m	47.03	100.75	259.02	165.74	166.71	776.67	12.82
36.00 m	369.25	1522.01	1842.45	88.11	99.63	552.40	37.65
37.30 m	98.75	342.10	467.86	184.93	202.48	973.34	17.32
38.30 m	74.85	267.27	581.22	79.35	127.25	728.78	15.59
39.60 m	87.67	257.07	570.29	144.81	166.08	1093.97	15.97
40.84 m	54.75	124.64	307.86	105.09	117.60	643.65	11.58
42.85 m	25.14	37.38	64.59	92.02	100.22	591.79	8.67
43.80 m	30.53	67.00	99.25	61.93	81.34	543.54	8.31
44.60 m	22.59	50.50	35.05	127.17	126.50	901.08	13.01
45.30 m	58.54	170.35	385.88	138.17	178.06	906.29	26.88
46.70 m	22.79	40.14	71.48	122.18	123.46	663.04	11.10
47.50 m	41.73	81.83	107.23	150.23	204.14	850.35	15.99
48.10 m	25.39	36.34	22.76	90.98	143.44	831.20	11.02
50.00 m	19.39	23.69	16.55	79.07	105.08	676.54	9.66
50.80 m	137.22	573.46	573.80	81.37	106.56	287.71	21.98
56.90 m	19.08	55.08	59.64	46.08	36.54	289.06	4.63
58.40 m	28.87	47.18	29.51	78.36	112.16	676.57	9.28
59.00 m	32.71	82.53	95.55	109.53	265.75	685.98	10.09
60.00 m	22.65	45.21	47.19	65.14	90.71	490.83	6.44
61.10 m	21.93	37.11	38.41	60.48	66.66	498.92	6.98

Lanka. The instrument was calibrated using standard ICP-MS calibration standard 2. The instrumental internal drift was corrected using 75 and 103 Rh as internal standards. Sample dilutions were made using deionized water. About a 25.0 cm long core to represent each meter of the mineralization has been selected and sawed to split in to half. A half core with approx. 25 cm in length was crushed in laboratory crusher and further crushed in a benchtop crusher to smaller grit size. The crushed rocks were then splitted using a splitter several times to get a reasonably sized sample for further grinding. Finally, about 10 gs of the carefully splitted sample was powdered in an agate mortar. A weight of 200 mg of finely powdered sample was digested in microwave digester using aqua regia acid mixture and prescribed procedures. Finally, sufficiently digested samples were filtered out and the solutions were diluted to the required levels and analyzed in ICP-MS.

4. Results and discussion

4.1. Salient features of field relations

In the mineralized zone, mainly two rock types were identified which are ultramafic host rock and intermediate basement rock (Fig. 3 and 4). According to the field relations, the ultramafic host rock may have apparently intruded into the intermediate basement rock. Both rocks show evidence for metamorphism under upper amphibolite to granulite facies conditions (see [27] for details).

4.2. Petrography

In the host rock and basement rock, veins enriched with secondary minerals are present in which sulfides, secondary magnetite and secondary mica are also found. In this Seruwila IOA deposit, mineralization has occurred at two phases which are (i) massive magnetitic sulfides that is formed in the earlier phase and (ii) secondary magnetite, sulfides and mica that has been formed at the later phase [40]. The host rock is highly altered, fractured and contains Labradorite with considerable amount and apatite generally formed as sub-rounded to oval grains.

4.3. Ultramafic host rock

Ultrabasic host rocks contain medium to coarse-grained clinopyroxene (25–35%), othopyroxene (10–15%), amphibole (10–20%), mica (biotite+phloghopite) (10–15%), feldspar (15–20%), chalcopyrite + pyrite (5–10%) and graphite (10–15%) as the dominant minerals with minor fine-grained magnetite and apatite. Quartz is presented very low amount or absent. The distribution of opaque mineral which is limited in these rocks. However, host rocks appear to have graded gabbroic affinities to monzonite. These rocks are highly altered and fractured weak rock by secondary minerals (Fig. 5f, 5 g and 5 h). Sericite, chlorite, tremolite, secondary mica, pyrite, chalcopyrite, secondary carbonate minerals are presented as filling material of micro-cracks and fractures. Rutile and zircon are presented as accessory minerals in ultramafic rock. Pyroxene could be observed as an abundant mineral in most of the thin sections studied containing both clinopyroxene and orthopyroxene in various proportions. In most of the thin sections, clinopyroxene content is higher than orthopyroxene content while few of them are dominant with orthopyroxene. Clinopyroxene generally form as medium to coarse grained texture (0.1–2.5 mm) with euhedral shape (Fig.5a, 5b and 5 g). Most of clinopyroxene grains carry amphibole, rutile, zircon and apatite inclusions while some are having free of inclusions. Othopyroxene grains generally form as medium to coarse grained (0.5–2 mm) anhedral crystals. Most of pyroxene grains show replacement by biotite and/ or hornblende along the fractures which indicate that the rock has been retrograded to the amphibolite facies (Fig.5f, 5 g, 5 h and 5i). Amphibole also were observed as an abundant mafic mineral in most of the thin sections. Amphiboles are observed mainly in two types, the first type is coarse grained (0.1–2 mm), pale green, euhedral amphibole crystals (Fig.5b). The second type is fine grained (<0.1 mm), brownish anhedral amphiboles (Fig.5d and 5i). The coarse grained euhedral amphiboles which are free of inclusions while fine-grained anhedral amphiboles which occur as inclusions in clinopyroxene. And secondary amphiboles are formed as a result of replacement of clinopyroxene grains.

Further, this rock contains both types of feldspar, plagioclase and alkali-feldspar as an abundant mineral. Plagioclase crystals are mostly medium to coarse (0.1– up to about 2 mm) grained, euhedral and having sharp grain boundaries. Most of plagioclase grains clearly show

Fig. 4. Macroscopic observations of the borehole core with log data.

polysynthetic twining. Sericite alteration is present along the cracks and along the twin lamellae in most of plagioclase grains. Alkali-feldspar is less in abundance when compared with plagioclase feldspar. Orthoclase can be found in the thin sections but microcline is very less abundant or absent. This rock contains both types of micas which are biotite, phlogopite and chlorite. Most of mica grains are subhedral, and anhedral grains are also present. All types of mica grains are randomly oriented. Grain size of biotite and phlogopite is varying from fine to medium (<0.1 mm to 3–4 mm) and most of grains have characteristic lath shape. Secondary biotite was occurred along the cleavages and edges of pyroxene, hornblende and primary biotite (Fig.5 h). Some biotite grains have been chloritized which indicates that the rock has been retrograded

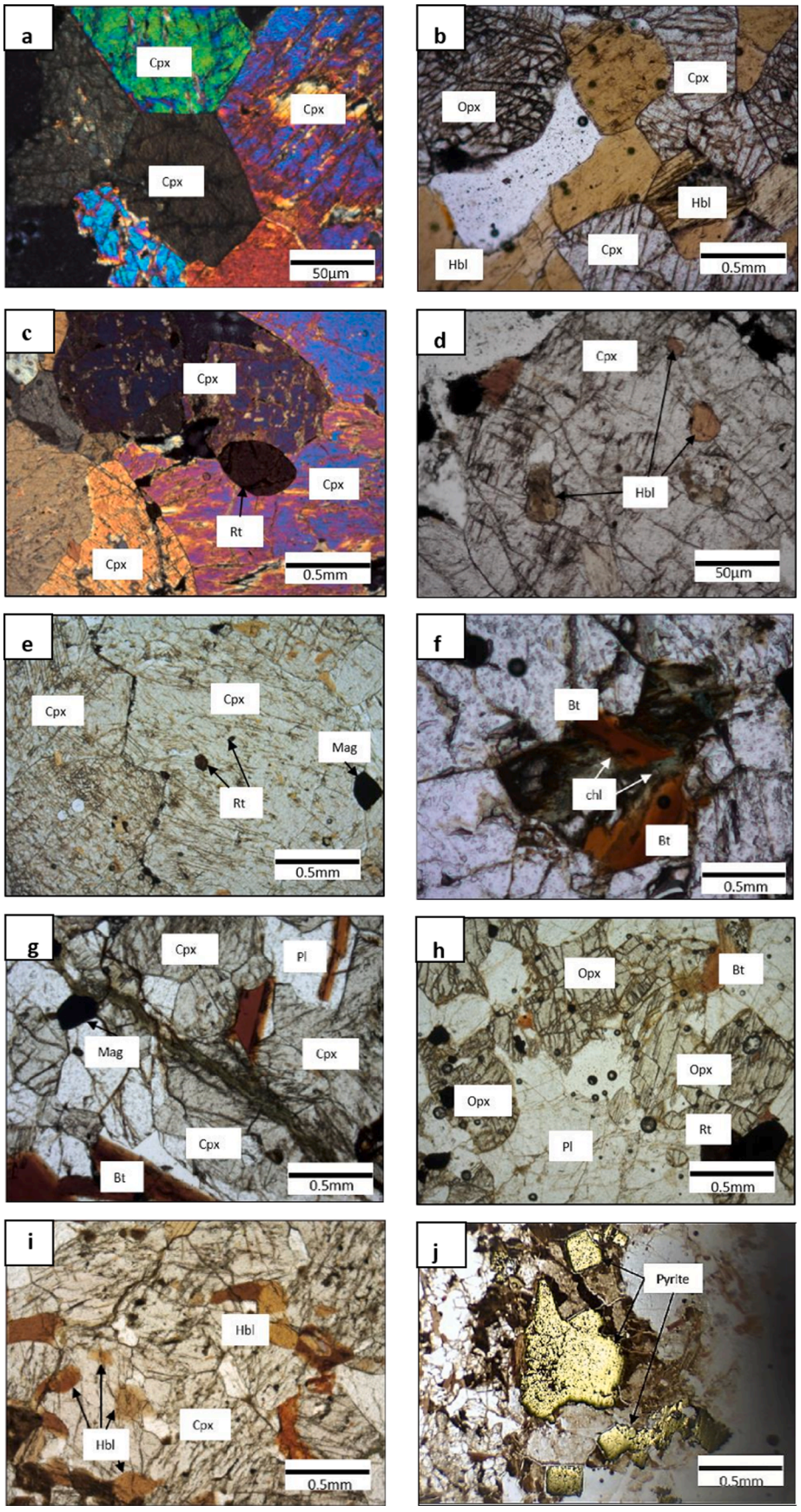

Fig. 5. Photomicrographs showing textures of representative samples of ultramafic host rock from Seruwila magnetite deposit. (**a**) cumulus texture including grain triple junctions and the large dihedral angle. (**b**)Euhedral amphibole which are free of inclusions. (**c**) Coarse-grained rutile crystals in matrix. (**d**)Fine grained anhedral amphiboles occur as inclusions in clinopyroxene. (**e**) Fine- grained rutile inclusions in the silicate minerals. (**f**) Biotite chloritization. (**g**) Fractures are filled with secondary minerals. (**h**) Most of othopyroxene grains show replacement by biotite along the fractures and grain margins. (**i**) Most of clinopyroxene grains show replacement by biotite and/ or hornblende along the fractures and grain margins. (**j**) Euhedral pyrite crystals in host rock.

to the Greenschist facies (Fig.5f). Chlorite grains occur as fine-grained (<0.1 mm) texture.

A minor amount of opaque phases contains in the ultrabasic host rocks. The main opaque mineral is magnetite, the distribution of which is limited in these samples. Magnetite occurs as fine to medium grained (<0.1 mm –1 mm), anhedral crystals with irregular morphology. Magnetite are distributed in thin sections as clusters in the matrix, as a filling material along the microcracks/fractures and, as a replacement material. Medium to coarse grained (0.1–1 mm), euhedral to subhedral pyrite crystals could be observed in the matrix while fine-grained pyrites could be observed along the microcracks and fractures as a filling material (Fig.5j). Rutile and zircon are present as accessory minerals in ultramafic rock. Two types of rutile grains are identified; the first is represented by coarse-grained anhedral crystals in the matrix and the

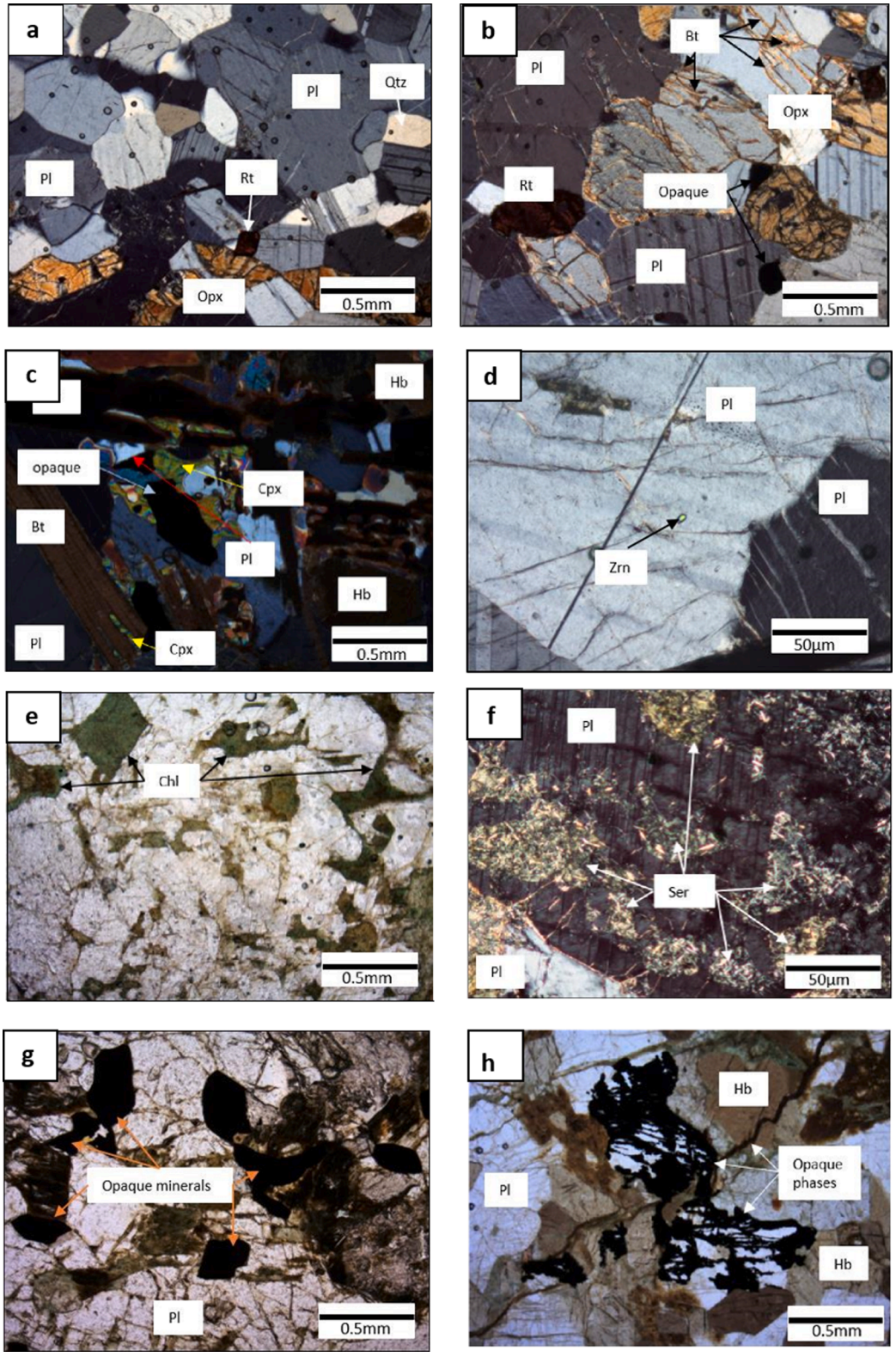

Fig. 6. Photomicrographs showing textures of representative samples of intermediate rock from Seruwila magnetite deposit. (**a**)Rutile grains and orthopyroxene grains in intermediate rock. (**b**)Biotite ateration at grain margins of orthopyroxene grains. (**c**) Clinopyroxene breakdown reaction. (**d**) Zircon grains generally occur as inclusions in the silicate minerals. (**e**) Chlorite alteration. (**f**) Sericite alteration. (**g**) Medium grained magnetite is the dominant opaque minerals. (**h**) Micro-cracks are filled with opaque minerals. Mineral abbreviations are after [99].

second type is fine-grained inclusions in silicate minerals (Fig.5e and 5 h). And also, Zircon grains generally occur as inclusions in the silicate minerals.

4.4. Intermediate rock

Intermediate rock contains medium to coarse-grained plagioclase (30–45%), pyroxene (10–15%), apatite (10%), biotite (10–15%), Quartz (10%) as the dominant minerals with minor fine-grained magnetite, amphibole. The most common accessory minerals encountered in these rocks are zircon and rutile. Zircons appear as fine-grained anhedral grains with varying grain sizes from 0.1 to 0.5 mm (Fig. 6d). Mafic mineral content in intermediate rock is relatively low. This rock consists of both clinopyroxene and orthopyroxene in various proportions. In this

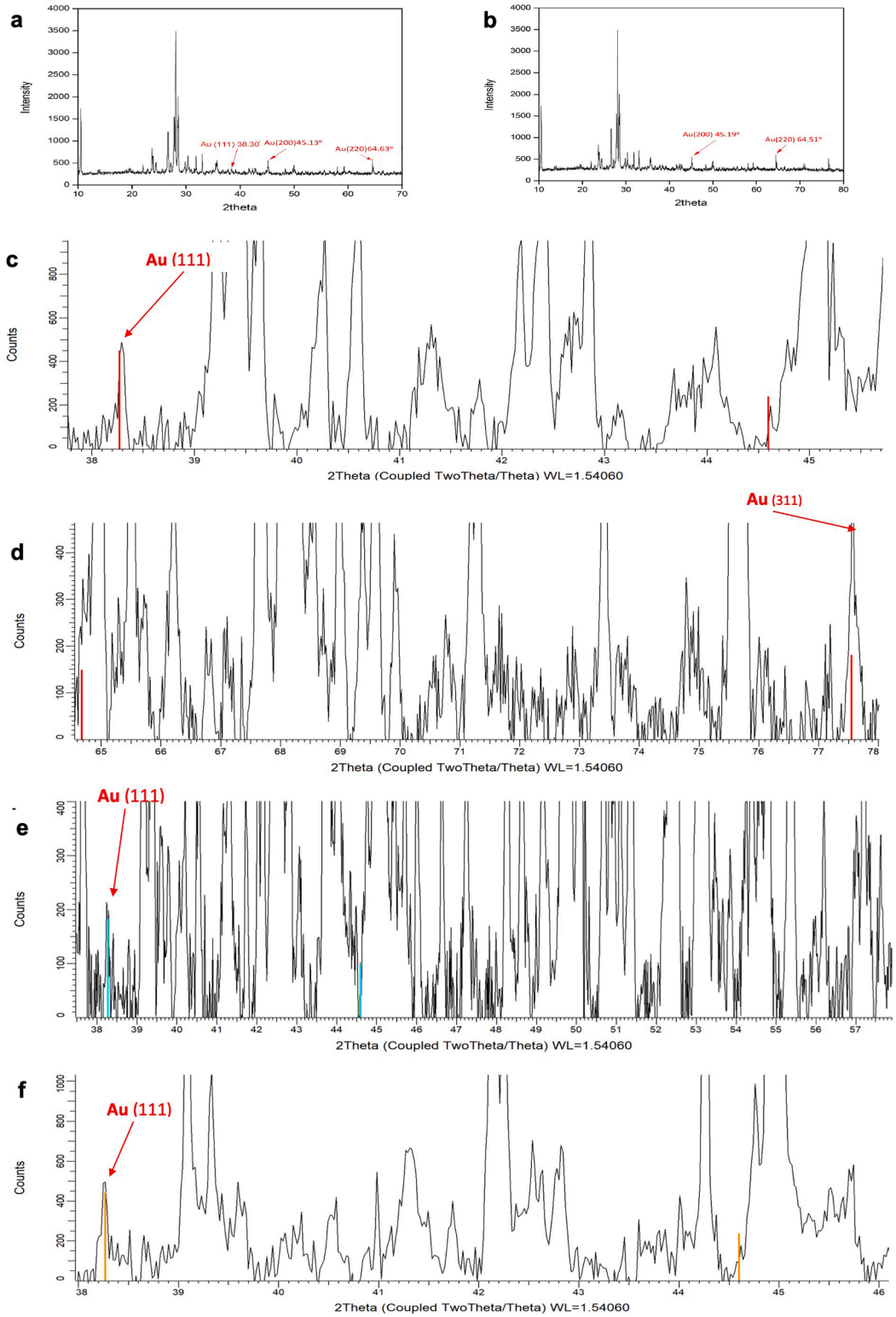

Fig. 7. XRD diffractogram of the sample from 36.00 m to 59.00 m depth.

rock, clinopyroxene content is higher than orthopyroxene content and clinopyroxene generally form as medium to coarse grained (0.1–2.0 mm) with anhedral crystals. Othopyroxene grains generally occur as medium to coarse grained (0.5–1 mm) anhedral crystals. Most of the pyroxene grains show replacement by biotite and/ or hornblende along the fractures.

This rock contains both types of feldspar, plagioclase, and alkali-feldspar. Plagioclase content is higher (more than 50%) than alkali-feldspar and microcline content is extremely less abundant or absent. Plagioclase crystals are mostly medium to coarse (0.1–2 mm) grained, euhedral to subhedral crystals (Fig. 6a and 6b). Most of plagioclase grains clearly show polysynthetic twining. Hornblende was observed as a minor mafic mineral in these rocks. Hornblende generally form as fine to medium grained (<0.1–0.5 mm), pale green, euhedral amphibole crystals (Fig. 6h). And secondary amphiboles are formed as a result of the replacement of clinopyroxene grains (Fig. 6c). Opaque phases contain very less amount in these rocks. The distribution of opaque phases is limited in these samples and which are distributed in thin sections as irregular clusters in the matrix and as a replacement material of among biotite, pyroxene, and hornblende (Fig. 6g and 6h). Rutile and zircon are present as accessory minerals in these rocks (Fig. 6a, 6b, and 6d). These rocks are highly altered and fractured weak rock by secondary minerals such as sericite, chlorite, secondary mica, and secondary carbonate minerals (Fig.6e, 6f and 6 h).

4.5. X-ray diffraction (XRD) analysis

XRD analysis is a unique analytical technique that is used for phase identification of crystalline material to determine mineral proportions of samples. Thirteen representative samples were analyzed using XRD (Fig. 7). The XRD data show the presence of graphite, quartz, anorthite, rutile, biotite with higher intensity count values varying in the range of 4000–100,000. The presence of graphite regards to metamorphic grade, a low-temperature character is indicated by the low degree of crystallinity of graphite. The general XRD diffractograms as detailed below clearly show high-intensity peaks, which are obtained by major silicates and minerals in the sample.

The intensity of Gold peaks is relatively low as observed in the studied samples compared with major silicates and other minerals. Therefore, gold peaks were detected by increasing peak resolution and broadening the diffractogram. In order to recognize gold peaks, a standard referenced XRD database (ICDD referenced database) was used. In the analyzed samples, low count values (50–500) were observed probably because the gold concentration is relatively low compared with the other minerals (Fig. 7). Gold peaks were detected in several samples (for example 27.00 m, 31.70 m, 46.70 m, 36.00 m, 59.00 m), and in few samples, elemental gold was entirely absent (for example: 45.30 m, 37.30 m, 53.61 m). However, the qualitative information obtained by the results convinces us that gold is present at least in some of the samples, though at low concentrations.

4.6. SEM analysis

Different areas of the sample were examined in dual mode (to see the images under both BSE and SEM modes). We also analyzed micro-cracks/veins and veinlets through SEM, however, physical detection of the presence of gold in the samples was difficult probably because gold concentration is relatively very low as inferred from XRD results (Fig. 8). Therefore, Au could be present as microscopically invisible, structurally-bonded particles and/or gold nanoparticles in the Seruwila mineral deposit.

4.7. Origin of the mineralization at Seruwila

As mentioned above, Seruwila iron oxide–apatite deposit is located at the contact between the Highland and Vijayan complexes. The general understanding is that this Kiruna-type deposit is formed during the late Neoproterozoic assembly of the Gondwana supercontinent (e.g. [27]). Most of the Kiruna type deposits are associated with intermediate to felsic rocks, and in rare cases with ultramafic rocks, similar to the ore deposit studied here, which is hosted in an ultramafic intrusion and comprises massive and disseminated mineralization. Some workers favor a magmatic model due to the close genetic relationship of the Kiruna-type magnetite–apatite mineralization with igneous suites , whereas others prefer a hydrothermal origin based on evidence from fluid inclusions, replacement texture, and metasomatic zones ([6]; [19]). Recent studies have proposed an integrated magmatic– hydrothermal model (e.g., [49,89,93]), which also confirms the genetic

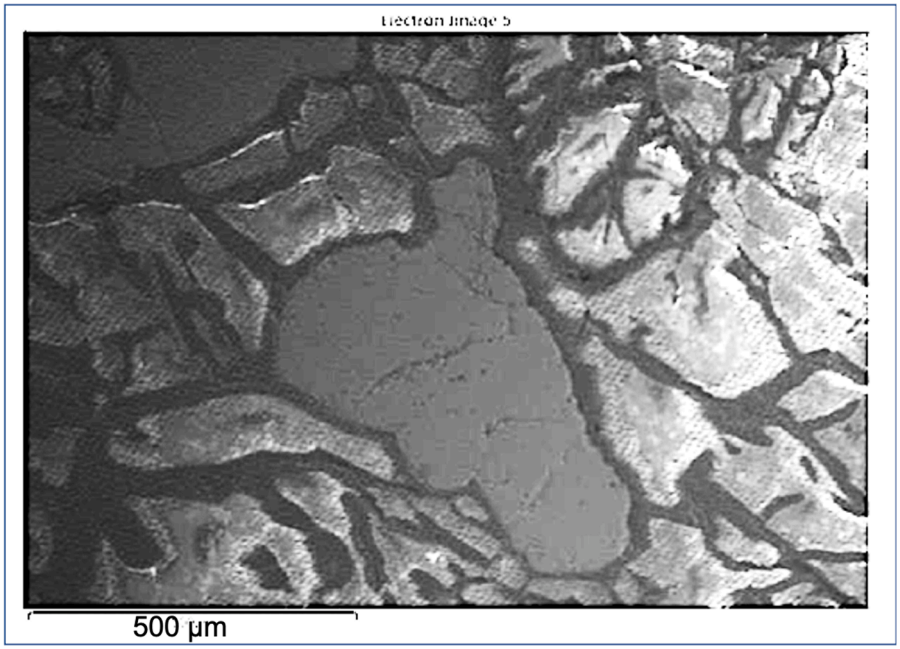

Fig. 8. SEM image showing the micro cracks around a rutile grain in the sample from 53.61 m depth.

connection between Kiruna-type IOA and iron oxide–copper–gold (IOCG) deposits, in which IOA deposits represent the deeper roots of the IOCG systems (e.g., [87]).

[27] suggested a magmatic–hydrothermal model for the mineralization wherein: (1) the Cl-rich magmatic–hydrothermal fluid scavenged Fe, and P from the ultramafic magma, transported iron to shallower levels in the crust and deposited along the suture zone to form the massive type magnetite and apatite; and (2) the progressive cooling of the hydrothermal fluids resulted in the growth of disseminated magnetite and the precipitation of sulfide minerals at a shallower level and trapped abundant fluid inclusions aided by the hydrothermal fluid at a shallower depth, forming the disseminated ore body, followed by calcic metasomatism (scapolitization and actinolitization). According to the results of ICP-MS analysis, typical Au-pathfinder elements also include in this deposit such as As, Cu, Pb, etc. Cu, Zn, Au, Ti, Pt, Cr, Ni, Zn, Mn, and Ba are also present in this deposit adding more economic value. In addition to Gold, mining may benefit because of the high concentrations of transition metals too. Further, this deposit is an alkaline type deposit because of the presence of Cu-Au±PGE association.

5. Conclusions

The rocks of the studied Seruwila deposit area are represented by the ultrabasic and intermediate intrusive rock domains and the ultrabasic rocks form abrupt contacts with the intermediate host. Our results indicate that metallic gold could be present in Seruwila IOA deposit, most probably associated with cracks within the rocks. However, exact occurrences, behavior and morphology of gold is not recognized yet. Detailed investigations are necessary along the veins, veinlets and on the surface of magnetite grains to quantify the Au mineralization in Seruwila IOA deposit, which is a promising target for future gold exploration. The veins present in the host rock help flow of ore-bearing fluids, precipitating gold and related (calcophile/siderophile) sulfides, most probably as structurally-bonded gold and/or gold nanoparticles. Accordingly, although ore-grade quantities of gold was not present in the current study, this ultrabasic rock at Seruwila can serve as a prospective guide for potential Au mineralization.

Acknowledgements

This is a contribution to the National Research Council (NRC), Sri Lanka, grant No: NRC 15–089 and Ministry of Science and Tecnology, Sri Lanka grant MTR/TRD/AGR/3/2/20. Ameca Lanka Ltd has generously provided us with the core samples for the study. Special thanks are extended to N.D. Subasinghe, Himal Wijekoon and Thilini Harischandra at NIFS, Kandy and Rashmi Rathnayake at SLINTEC, Homagama for sample preparations and analytical helps, respectively. All the reviewers and Prof. K. Sajeev at the Indian Institute of Science, Bangalore are highly acknowledged for constructive comments.

References

[1] G. Ai, T. Dai, M. Chen, Typomorphic characteristics and occurrence of gold of pyrite-arsenopyrite-antimonite in gold deposit: a case study of the gold deposits in Hunan Province, Geol. Resour.s 19 (2010) 157–163.
[2] G.B. Arehart, S.L. Chryssoulis, S.E. Kesler, Gold and arsenic in iron sulfides from sediment-hosted disseminated gold deposits; implications for depositional processes, Econ. Geol. 88 (1993) 171–185.
[3] P. Ashley, C. Creagh, C. Ryan, Invisible gold in ore and mineral concentrates from the Hillgrove goldantimony deposits, NSW, Australia, Miner. Deposita 35 (2000) 285–301.
[4] B.M. Bakken, M.F. Hochella, A. Marshall, Highresolution microscopy of gold in unoxidized ore from the Carlin Mine, Nevada, Econ. Geol. 84 (1989) 171–179.
[5] Z. Bao, R. Wan, J. Bao, Typomorphic characteristics and occurrence of gold in arsenopyrite in the gold deposit, Yunnan Geol. 24 (2005) 32–48.
[6] M.D. Barton, D.A Johnson, Evaporitic-source model for igneous-related Fe oxide–(REE-Cu-Au-U) mineralization, Geology 24 (3) (1996) 259–262.
[7] N. Baur, A. Kröner, W. Todt, T.C. Liew, A.W. Hofman, U–Pb isotopic systematics of zircons from prograde and retrograde transition zones in high grade orthogneisses, Sri Lanka, J. Geol. 99 (1991) 527–545.
[8] R. Belcher, A. Rozendaal, W. Przybylowicz, Trace element zoning in pyrite determined by PIXE elemental mapping: evidence for varying ore–fluid composition and electrochemical precipitation of gold at the Spitskop deposit, Saldania Belt, South Africa, X-Ray Spectrom. 33 (2004) 174–180.
[9] A.R. Berger, N.R. Jayasinghe, Precambrian structure and chronology in the highland series of Sri Lanka, Precambrian Res 3 (1976) 559–576.
[10] S.J. Bi, J.W. Li, M.F. Zhou, Z.K. Li, Gold distribution in As-deficient pyrite and telluride mineralogy of the Yangzhaiyu gold deposit, Xiaoqinling district, southern North China craton, Miner. Deposita 46 (2011) 925–941.
[11] I. Braun, L.M. Kriegsman, Proterozoic crustal evolution of southernmost India and Sri Lanka, Geol. Soc. London Spec. Publ. 206 (2003) 169–202.
[12] R.R. Brooks, A.J.M. Baker, R.S. Ramakrishna, D.E. Ryan, Botanical and geochemical exploration studies at the seruwila copper-magnetite prospect in Sri Lanka, J Geochem Explor 24 (1985) 223–235.
[13] G. Büchel, Gravity, magnetic and structural patterns at the deep-crustal plate boundary zone between West- and East-Gondwana in Sri Lanka, Precambrian Res. 66 (1994) 77–91.
[14] K. Burton, R. O'Nions, Fe-Ti oxide chronometry: with application to granulite formation, Geochim. Cosmochim. Acta 54 (1990) 2593–2602.
[15] P.G. Cooray, An Introduction to the Geology of Sri Lanka, 340, National Museum Sri Lanka Publication, 1984.
[16] P.G. Cooray, The Precambrian of Sri Lanka: a historic review, Precambrian Res 66 (1994) 3–18.
[17] K. Dahanayake, H.A.K. Jayasena, General geology and petrology of somePrecambrian crystalline rocks from the Vijayan Complex of Sri Lanka, Precambrian Res. 19 (1983) 301–315.
[18] K. Dahanayake, Structural and petrological studies on the Precambrian Vijayan Complex of Sri Lanka, Revista Brasiliana Geociencias 12 (1982) 89–93.
[19] S.A.S. Dare, S. Barnes, G. Beaudoin, Did the massive magnetite "lava flows" of El Laco (Chile) form by magmatic or hydrothermal processes? New constraints from magnetite composition by LA-ICP-MS, Miner. Deposita 50 (2015) 607–617.
[20] P.L. Dharmapriya, S.P.K. Malaviarachchi, M. Santosh, L. Tang, K. Sajeev, Late-Neoproterozoic ultrahigh temperature metamorphism in the Highland Complex, Sri Lanka, Precambrian Res 271 (2015) 311–333.
[21] C.B. Dissanayake, T. Munasinghe, Reconstruction of the Precambrian sedimentary basin in the Granulite belt of Sri Lanka, Chem. Geol. 47 (1984) 221–247.
[22] C.B. Dissanayake, S.V.R. Weerasooriya, Fluorine as an indicator of mineralization—Hydrogeochemistry of a Precambrian mineralized belt in Sri Lanka, Chem. Geol. 56 (1986) 257–270.
[23] D. Eliopoulos, S. Skounakis, M. Economou-Eliopoulos, Geochemical characteristics of sulfide mineralizations from the Pindos ophiolite complex, Bulletin of the Geol. Soc. Greece, XXXII, 3 (1998) 179–186.
[24] S. Faulhaber, M. Raith, Geothermometry and geobarometry of high-grade rocks: a case study on garnet-pyroxene granulites in Southern Sri Lanka, Mineral. Mag. 55 (1991) 33–56.
[25] T. Hatherton, D.B. Pattiarachchi, V.V.C. Ranasinghe, Gravity Map of Sri Lanka, 1: 1,000,000, Geol. Surv. Department, Sri Lanka (1975) 39. Profesional Paper 3.
[26] P. Hazarika, B. Mishra, S. Saravanan Chinnasamy, et al., Multi-stage growth and invisible gold distribution in pyrite from the Kundarkocha sediment-hosted gold deposit, eastern India, Ore Geol Rev 55 (2013) 134–145.
[27] X.F. He, M. Santosh, T. Tsunogae, S.P.K. Malaviarachchi, P.L. Dharmapriya, Neoproterozoic arc accretion along the "eastern suture" in Sri Lanka during Gondwana assembly, Precambrian Res 279 (2016) 57–80, https://doi.org/10.1016/j.precamres.2016.
[28] X.F. He, M. Santosh, T. Tsunogae, S.P.K. Malaviarachchi, Magnetiteapatite deposit from Sri Lanka: implications on Kiruna-type mineralization associated with ultramafic intrusion and mantle metasomatism, Am. Mineral. 103 (2018) 26–38, pages2018.
[29] He, X.-F., Santosh, M., Tsunogae, T., Malaviarachchi, S.P.K., 2015. Early to late Neoproterozoic magmatism and magma mixing–mingling in Sri Lanka: implications for convergent margin processes.
[30] R.E. Healy, P. William, Petrology of Au-Ag-Hg alloy and 'invisible' gold in the Trout lake massive sulfide deposit, Flin Flon, Manitoba, Canad. Mineral. 28 (1990) 189–206.
[31] N. Herz, L.B. Valentine, Rutile in the Harford Country, Maryland, serpentine belt. U.S. Geol. Surv. Profess. Paper 700-C, 1970, pp. 43–48.
[32] R.S. Hilderband, Kiruna-type deposits: their origin and relationship to intermediate subvolcalic plutons in the Great Bear magmatic zone, Northwest Canada, Econ. Geol. 8 (1986) 640–659.
[33] Y. Hiroi, Y. Ogo, K. Namba, Evidence for prograde metamorphic evolution of Sri Lankan pelitic granulites, and implications for the development of continental crust, Precambr. Res. 66 (1994) 245–263.
[34] M.W. Hitzman, N. Oreskes, M.T. Einaudi, Geological characteristics and tectonic setting of Proterozoic iron oxide (Cu-U-Au-REE) deposits, Precambrian Res 58 (1992) 241–287, v.
[35] S. Hölzl, H. Köhler, A. Kröner, P. Jaeckel, T.C. Liew, Geochronology of the Sri Lankan Basement. Geol. Surv. Department, Sri Lanka, 1991, pp. 237–257. Professional Paper 5.
[36] S. Hölzl, A.W. Hofmann, W. Todt, H. Köhler, U–Pb geochronology of the Sri Lankan basement, Precambrian Res. 66 (1994) 123–149.
[37] L. Hopkinson, S. Roberts, Ridge axis deformation and coeval melt migration within layer 3 gabbros: evidence from the Lizard complex, U.K, Contrib. Mineral. Petrol. 121 (1995) 126–138.
[38] T. Hou, Z. Zhang, J. Encarnacion, H. Huang, M. Wang, Geochronology/geochemistry of the Washan dioritic porphyry associated with Kiruna-type iron

ores, Middle-Lower Yangtze River Valley, eastern China: implications for petrogenesis/mineralization, Int. Geol. Rev. 54 (2012) 1332–1352.
[39] M.B. Holness, M.J. Cheadle, D McKenzie, On the use of changes in dihedral angle to decode late-stage textural evolution in cumulates, J. Petrol. 46 (2005) 1565–1583.
[40] D.E. Jayawardena, The geology and tectonic setting of the copper-lron ore prospect at Seruwila—North East Sri Lanka, J. Natl. Sci. Council Sri Lanka 10 (1982) 129–142.
[41] E. Jonsson, V.R. Troll, K. Högdahl, C. Harris, F. Weis, K.P. Nilsson, A. Skelton, Magmatic origin of giant "Kiruna-type" apatite-iron-oxide ores in central Sweden, Sci Rep 3 (2013) 1644.
[42] Jose Antonio Cirillo De Assis, George Luiz Luvizotto, Gold deposits in poly-deformed metasedimentary rocks: a case study of the C1-Santaluz gold deposit, Itapicuru Greenstone Belt, Northeast of Brazil, Braz. J. Geol. 48 (4) (2018) 651–670.
[43] K.V.W. Kehelpannala, Deformation of a high-grade Gondwana fragment, Sri Lanka, Gondwana Res. 1 (1997) 47–68.
[44] K.V.W. Kehelpannala, Structural evolution of the middle to lower crust in Sri Lanka—A review, J. Geol. Soc. Sri Lanka 11 (2003) 45–86.
[45] K.V.W. Kehelpannala, Arc accretion around Sri Lanka during the assembly ofGondwana, Gondwana Res. 7 (2004) 41–46.
[46] R. Kleinschrodt, G. Voll, W. Kehelpannala, A layered basic intrusion, deformed and metamorphosed in granulite facies of the Sri Lanka basement, Int. J. Earth Sci. 80 (1991) 779–800.
[47] R. Kleinschrodt, Large scale thrusting in the lower crustal basement of Sri Lanka, Precambrian Res. 66 (1994) 39–57.
[48] R. Kleinschrodt, Strain localization and large-scale block rotation in the lower continental crust, Kataragama area, Sri Lanka, Terra Nova 8 (3) (1996) 236–244.
[49] J.L. Knipping, L.D. Bilenker, A.C. Simon, M. Reich, F. Barra, A.P. Deditius, C. Lundstrom, I. Bindeman, R. Munizaga, Giant Kiruna-type deposits form by efficient flotation of magmatic magnetite suspensions, Geology 43 (2015) 591–594.
[50] L.M. Kriegsman, J.C. Schumacher, Petrology of sapphirine-bearing and associated granulites from central Sri Lanka, J. Petrol. 40 (1999) 1211–1239.
[51] L.M. Kriegsman, The Pan-African event in East Antarctica: a view from Sri Lanka and the Mozambique belt, Precambrian Res. 75 (3) (1995) 263–277.
[52] A. Kröner, P. Jaeckel, Zircon ages from rocks of the Wanni Complex, Sri Lanka, J. Geol. Soc. Sri Lanka 5 (1994) 41–57.
[53] A. Kröner, P.G. Cooray, P.W. Vitanage, Lithotectonic subdivision of the Precambrian basement in Sri Lanka, Geol. Surv. Department, Sri Lanka, Profess. Paper 5 (1991) 5–21.
[54] A. Kröner, K.V.W. Kehelpannala, E. Hegner, Ca. 750–1100 Ma magmatic events and Grenville-age deformation in Sri Lanka: relevance for Rodinia supercontinent formation and dispersal, and Gondwana amalgamation, J. Asian Earth Sci. 22 (2003) 279–300.
[55] A. Kröner, Y. Rojas-Agramonte, K.V.W. Kehelpannala, T. Zack, E. Hegner, H. Y. Geng, J. Wong, M. Barth, Age, Nd-Hf isotopes, and geochemistry of the Vijayan Complex of eastern and southern Sri Lanka: a Grenville-age magmatic arc of unknown derivation, Precambr. Res. 234 (2013) 288–321.
[56] A. Kröner, I.S. Williams, W. Compston, N. Baur, P.W. Vithanage, L.R.K. Perera, Zircon ion microprobe dating of high grade rocks in Sri Lanka, J. Petrol. 95 (1987) 775–791.
[57] R.R. Large, L. Danyushevsky, C. Hollit, V. Maslennikov, S. Meffre, S. Gilbert, S. Bull, R. Scott, P. Emsbo, H. Thomas, Gold and trace element zonation in pyrite using a laser imaging technique: implications for the timing of gold in orogenic and Carlin-style sediment-hosted deposits, Econ. Geol. 104 (2009) 635–668.
[58] S.P.K. Malaviarachchi, A. Takasu, Electron microprobe dating of monazites from Sri Lanka, J. Geol. Soc. Sri Lanka 14 (2011) 81–90.
[59] S.P.K. Malaviarachchi, P.L. Dharmapriya, Revisiting Ultrahigh Temperature granulites of Sri Lanka: new prograde and retrograde mineral textures from the Highland Complex, J. Indian Inst. Sci. (2015).
[60] V. Mathavan, G.W.A.R. Fernando, Reactions and textures in grossular-wollastonite-scapolite calc-silicate granulites from Maligawila, Sri Lanka: evidence for hightemperature isobaric cooling in the meta-sediments of the Highland Complex, Lithos 59 (2001) 217–232.
[61] V. Mathavan, K.B.N. W., W.K.B.N. Prame, P.G. Cooray, Geology of the high grade Proterozoic terrains of Sri Lanka and the assembly of Gondwana: an update on recent developments, Gondwana Res. 2 (1999) 237–250.
[62] C.C. Milisenda, T.C. Liewa, A.W. Hoffmanna, A. Kröner, Isotopic mapping of age provinces in Precambrian high-grade terrains: Sri Lanka, J. Geol. 96 (1988) 608–615.
[63] C.C. Milisenda, T.C. Liewa, A.W. Hofmanna, H. Köhler, Nd isotopic mapping of the Sri Lanka basement: update, and additional constraints from Sr isotopes, Precambrian Res 66 (1994) 95–110.
[64] C.C. Milisenda, J.R. Pohl, A.W. Hofmanna, Charnockite formation at Kurunegala, Sri Lanka. Geological Survey Department, Sri Lanka, Profess. Paper 5 (1991) 141–149.
[65] T. Munasinghe, C.B. Dissanayake, A plate tectonic model for the geologic evolution of Sri Lanka, J. Geol. Soc. India 23 (1982) 369–380.
[66] J.O. Nyström, F. Henriquez, Magmatic features of iron ores of the Kiruna-type in Chile and Sweden: ore textures and magnetite geochemistry, Econ. Geol. 89 (1994) 820–839.
[67] Y. Osanai, K. Sajeev, M. Owada, K.V.W. Kehelpannala, W.K.B. Prame, N. Nakano, S. Jayatileke, Metamorphic evolution of high-pressure and ultrahigh-temperature granulites from the Highland Complex, Sri Lanka, J. Asian Earth Sci. 28 (2006) 20–37.
[68] Y. Osanai, A.K. Tsutomu, Y. Miyashita, I. Kusachi, T. Yamasaki, D. Doyama, W.K. B.N. Prame, S. Jayatileke, V. Mathavan, Geological fieldwork in the southwestern and central parts of the highland complex, Sri Lanka, during 1998–1999, with special reference to the highest grade metamorphic rocks, J. Geosci. 43 (2000) 227–247.
[69] C.S. Palenik, S. Utsunomiya, M. Reich, S.E. Kesler, L. Wang, R.C. Ewing, Invisible"gold revealed: direct imaging of gold nanoparticles in a Carlin-type deposit, Am. Mineral. 89 (2004) 1359–1366.
[70] D.W. Pals, P.G. Spry, S. Chryssoulis, Invisible gold and tellurium in arsenic-rich pyrite from the Emperor gold deposit, Fiji: implications for gold distribution and deposition, Econ. Geol. 98 (2003) 479–493.
[71] H.D.N.C. Pathirana, Geology of Sri Lanka in relation to plate tectonics, J. Natl. Sci. Council of Sri Lanka 8 (1) (1980) 75–85.
[72] L.R.K. Perera, Co-existing cordierite-almandine-a key to the metamorphic history of Sri Lanka, Precambr. Res. 25 (1984) 349–364.
[73] J.G. Pohl, R. Emmermann, Chemical Composition of the Sri Lanka Precambrian Basement. Geol. Surv. Department, Sri Lanka, 1991, pp. 94–123. Professional Paper 5.
[74] W. Prame, Metamorphism and nature of the granulite-facies crust in southwestern Sri Lanka: characterization by pelitic/psammopelitic rocks and associated, Summ. Res. Ger. Lankan Consort. 827 (1991) 188–199.
[75] P. Raase, V. Schenk, Petrology of granulite-facies metapelites of the Highland Complex, Sri Lanka: implications for the metamorphic zonation and the P-T path, Precambr. Res. 66 (1994) 265–294.
[76] A.U. Rajapaksha, M. Vithanage, C. Oze, W.M.A.T. Bandara, R. Weerasooriya, Nickel and manganese release in serpentine soil from the Ussangoda Ultramafic Complex, Sri Lanka, Geoderma 189–190 (2012) 1–9.
[77] A. Sabet-Mobarhan-Talab, F. Alinia, S.S. Ghannadpour, A. Hezarkhani, Geology, geochemistry, and some genetic discussion of the Chador- Malu iron oxide-apatite deposit, Bafq District, Central Iran, Arabian J. Geosci. 8 (2015) 8399–8418.
[78] K. Sajeev, Y. Osanai, Osumilite and spinel+quartz from Sri Lanka: implications for UHT conditions and retrograde P-T path, J. Mineral. Petrol. Sci. 99 (2004) 320–327.
[79] K. Sajeev, Y. Osanai, Ultrahigh-temperature Metamorphism (1150°C, 12 kbar) and Multistage Evolution of Mg-, Al-rich Granulites from the Central Highland Complex, Sri Lanka, J. Petrol. 45 (2004) 1821–1844.
[80] K. Sajeev, Y. Osanai, J.A.D. Connolly, S. Suzuki, J. Ishioka, H. Kagami, S. Rino, Extreme Crustal Metamorphism during a Neoproterozoic Event in Sri Lanka: a Study of Dry Mafic Granulites, J. Geol. 115 (2007) 563–582.
[81] M. Sandiford, R. Powell, S.F. Martin, L.R.K. Perera, Thermal and baric evolution of garnet granulites from Sri Lanka, J. Metamorph. Geol. 6 (1988) 351–364.
[82] M. Santosh, T. Tsunogae, Malaviarachchi, P.K. Sanjeewa, Z.M. Zhang, H.X. Ding, L. Tang, P.L. Dharmapriya, Neoproterozoic crustal evolution in Sri Lanka: insights from petrologic, geochemical and zircon U–Pb and Lu–Hf isotopic data and implications for Gondwana assembly, Precambrian Res 255 (2014) 1–29.
[83] S. Seneviratne, The ecology and archaeology of the Seruwila Copper- Magnetite Deposit, North East Sri Lanka. The Sri Lanka Journal of the Humanities, 21, 114–145. microanalysis, Chem. Geol. 249 (1995) 1–35.
[84] V. Schenk, P. Raase, R. Schumacher, Metamorphic zonation and PT history of the Highland Complex in Sri Lanka, Cryst. crust Sri Lanka Part I (1991) 150–163.
[85] R. Schumacher, S. Faulhaber, Summary and discussion of P-T estimates from garnet-pyroxene-plagioclase-quartz-bearing granulite-facies rocks from Sri Lanka, Precambr. Res. 66 (1994) 295–308.
[86] Schumacher, R., Schenk, V., Raase, P., 1990. In: High-Temperature Metamorphism and Crustal Anatexis, pp. 235–271.
[87] R.H. Sillitoe, Iron oxide–copper–gold deposits: an Andean view, Mineral Deposits 38 (2003) 787–812.
[88] Y.-.H. Sung, J. Brugger, C.L. Ciobanu, et al., Invisible gold in arsenian pyrite and arsenopyrite from a multistage Archaean gold deposit: sunrise Dam, Eastern Goldfields Province, Western Australia, Miner. Deposita 44 (2009) 765–791.
[89] S. Taghipour, A. Kananian, D. Harlov, R. Oberhänsli, Kiruna-type iron oxide-apatite deposits, Bafq District, Central Iran: fluid-aided genesis of fluorapatite-monazite-xenotime assemblages, Can Mineral 53 (2015) 479–496.
[90] Y. Takamura, T. Tsunogae, M. Santosh, S.P.K. Malaviarachchi, Y. Tsutsumi, UPb geochronology of detrital zircon in metasediments from Sri Lanka: implications for the regional correlation of Gondwana fragments, Precambr. Res. 281 (2016) 434–452.
[91] Y. Takamura, T. Tsunogae, M. Santosh, S.P.K. Malaviarachchi, Y. Tsutsumi, Petrology and zircon U-Pb geochronology of metagabbro from the Highland Complex, Sri Lanka: implications for the correlation of Gondwana suture zones, J. Asian Earth Sci. 113 (2015) 826–841.
[92] V.L. Tauson, Gold solubility in the common gold-bearing minerals; experimental evaluation and application to pyrite, Eur. J. Mineral. 11 (1999) 937–947.
[93] F. Tornos, F. Velasco, J.M. Hanchar, C.D. Astrobiología, C.C. Torrejón, T. D. Ardoz, Iron-rich melts, magmatic magnetite, and superheated hydrothermal systems: the El Laco deposit, Chile. Geol. 44 (2016) 427–430.
[94] Vaughan, J., & Kyin, A. (2004). Refractory gold ores in Archaean greenstones, Western Australia: mineralogy, gold paragenesis, metallurgical characterization and classification. Mineral Mag, 68, 255–277.
[95] P.W. Vitanage, Tectonics and mineralization in Sri Lanka, Bull. Geol. Soc. Finland 57 (1985) 157–168.
[96] P.W. Vitanage, Post-Precambrian uplift and regional neotectonic movements in Ceylon, in: 24th International Geological Congress, Montreal, Section 3, 1972, pp. 642–654.
[97] G. Voll, R. Kleinschrodt, Sri Lanka: structural, magmatic and metamorphic development of a Gondwana fragment, in: A. Kröner (Ed.), Sri Lanka: structural,

magmatic and metamorphic development of a Gondwana fragment, The Crystalline Crust of Sri Lanka, Part I. Summary of Research of the German-Sri Lankan Consortium (1991) 22–52. Professional Paper 5.
[98] G. Von Gruenewaldt, Ilmenite-apatite enrichment in the upper zone of the Bushveld Complex: a major titanium-rock phosphate resource, Int. Geol. Rev. 35 (1994) 987–1000.
[99] D.L. Whitney, B.W. Evans, Abbreviations for names of rock-forming minerals, Am. Mineral. 95 (2010) 185–187.
[100] M. Willbold, E. Hegner, R. Kleinschrodt, H.-.G. Stosch, K.V.W. Kehelpannala, P. Dulski, Geochemical evidence for a Neoproterozoic magmatic continental margin in Sri Lanka-relevence for the Rodinia-Gondwana supercontinental cycle, Precambrian Res. 130 (2004) 185–198.
[101] J. Zachariáš, J. Frýda, B. Paterová, M. Mihaljevič, Arsenopyrite and As-bearing pyrite from the Roudný deposit, Bohemian Massif, Mineral Mag 68 (2004) 31–46.
[102] Y. Zhang, T. Kusky, L. Wang, J. Li, P. Feng, Y. Huang, R. Giddens, Occurrence of gold in hydrothermal pyrite, western Taupo Volcanic Zone, New Zealand, Geodinamica Acta 28 (3) (2015) 185–198, 2016.
[103] Sanjeewa Malaviarachchi P.K, Satish M Kumar, Toshiro Takahashi, et al., New Sr-Nd Isotope Data Record Juvenile and Ancient Crust-Mantle Melt Interactions in the Vijayan Complex, Sri Lanka, Journal of Geology 129 (2021), https://doi.org/10.1086/714172.
[104] L.R.K Perera, Co-existing cordierite-almandine – a key to the metamorphic history of Sri Lanka. Precambrian Research 25 (1984) 349–364.